Study of Adaptive Grid Method Contribution in Flow Visualization with Effects of Supersonic Invisicd Flow over Wedge Parameters

Dr. Eng. Saad Sabah
Karam
E-mail:
alraneensc@yahoo.com

ABSTRACT

The effects of the use of different adaptive gird methods are investigated of supersonic inviscid 2-D external flow over two different shapes of wedge of different angle of attacks. For viscous flow solution, the effects of adaptations are invistaged for different turbulence model usage. Hyperbolic grid generation program built to generate the structured grid for 2-D viscous flow problem. For supersonic 2-D inviscid flow, the use of r-refinement grid adaption algorithm is used to develop the solution of Euler PDE with the use of MacCormak finite different solver. Fortran 99 program built for elliptic and hyperbolic grid generation and MacCormak 2-D solver which are fed to grid adaption program. Results showed correction , increase in accuracy , time saving for 2-D flows as a results of both r-refinement and h-refinement adaptaion algorithm implementation.

Keywords

Adaptive grid , adaption, wedge flow , flow visualization .

Nomenclature

a	Speed of sound
$C\xi$, $C\eta$, $C\phi$	Artificial viscosity coefficient in ξ, η and ϕ direction respectively
D	Van driest damping factor
e	Specific internal energy per unit mass
Et	Total energy per unit volume
E, F, G	Column vector in Cartesian coordinate
$\vec{E}, \vec{F}, \vec{G}$	Column vector in body fitted coordinate
E1, E2, E3, E4	Vector
U1, U2, U3, U4	Vector
I	Identity matrix
Imax	Number of grid points in ξ direction
Jmax	Number of grid points in η direction
Kmax	Number of grid points in ϕ direction
K	Coefficient of thermal conductivity
KT	Turbulent thermal conductivity
M	Mach number
M	Mass flow rate
P	Static pressure
$p\infty$	Free stream pressure
p0	Stagnation pressure
Pr	Molecular prandtl number
prt	Turbulent prandtl number
Re	Reynolds's number
$Re\Delta x$, $Re\Delta y$	Reynolds's number per step size in x and y respectively
ω	Relaxation parameter
γ	Ratio of specific heat , $\gamma = 1.4$
Δt	Time step
ρ	Density
Δ	Denotes an increment of the variable that follows
μ	Viscosity factor
μr	Turbulent viscosity factor
α	Flow angle of attack
Δx , Δy , Δz	Spatial steps in physical domain
$\Delta\xi$, $\Delta\eta$, $\Delta\phi$	Spatial steps in computational domain
ξ , η , ϕ	Computational coordinates

1. INTRODUCTION

In this study, the effect of flow over 2-D wedge will be investigated. The flow over wedge is considered as a case study and two dimensional, subsonic inviscid flows were studied. Both h-refinement and r-refinement adaption will be considered. Additionally, the resolution will be examined by changing the turbulence modeling parameter depending to the used mesh in the solution viscous flow problems. Previous of grid adaptation paper and study this case, Berger [1] presented a method of adaptive grid refinement for the solution of Euler equation for transonic external flow and studied the external flow over NACA 0012 aerofoil. And Eiseman [2] developed an alternating direction method for flow over a biconvex

aerofoil that adaptively resolve numerical solutions to physical problems by moving the points of a coordinate grid and illustrated his used weighting function with a parabolic disturbance occurring in the flow over the studied biconvex aerofoil. And Shen, [3] studied a depth-averaged two-dimensional model uses the solution – adaptive grid method to adapt the distribution of the computational grid point based on the newly computed field variables during simulation. Borsboom [4] presented the first technique of a moving adaptive grid technique for any arbitrary flow and transport problems that is based on the approximate minimization in the L-1 norm of the modeling error due to discertization, he considered only an analytical grid with pure mathematical model. These numerical methods used to solve the flow over wedge shaped geometries. Littlefield et al, [5] described the implementation of an adaptive mesh refinement scheme into an existing two and three dimensional Eulerian hydrocode which solve a problem of internal supersonic flow in a square cross section duct. The method of adaptation is illustrated by the refinement of a parent cell into eight child cells. Azarenok and Ivanenko, [6] coupled the solution – adaptive grid generation procedure with the Godunov- type solver for the second order accuracy.The researchers studied the supersonic internal flow in wind tunnel having square cross section area, the flow faces a back-facing step which enlarges the wind tunnel section area. They concluded that dynamically adaptive grids, clustered to singularities, allow increasing accuracy of numerical solution. Pimental etal [7] presented the result of a numerical study of premixed hydrogen-air flows ignition by an oblique shock wave (OSW) stabilized by a wedge, in situation when initial and boundary conditions are such that transition between the initial OSW and an oblique detonation wave (ODW) is observed. Computation performed using an adaptive, unstructured grid, finite volume computer code previously developed for the sake of the computations of high speed, compressible flows of reactive gas mixtures. And Eman A. Salih, [8] introduced numerical solution of supersonic inviscid and viscous compressible fluid flow over a vane with different angle of attack. In the viscous flow a full Navier-Stock equations was solved using explicit time marching Mackormak predictor – corrector technique. This method was used to solve two-dimensional viscous flow over the vane. Baldwin – Lomax turbulence model was used to study the viscous effect. Different flow conditions were tested with different Mach numbers up to 7. The method revealed a good match with the previous works.

2. Problem statement and governing equations

The geometry of the problem consists two type of wedge as shown in figure (1). And a simple schematic diagram for boundary conditions for the problem showing in figure (2). The mathematical statement for this problem basic on the physical principles of fluid dynamics equation Conservation of mass, Conservation of momentum (Newton's second low of motion) and Conservation of energy. The mathematical representation of the governing equations for an unsteady three dimensional, compressible, viscous flows in conservative form for neglected body forces are:

Continuity equation

$$\frac{\partial \rho}{\partial t} + \nabla.(\rho V) = 0 \qquad (2.1)$$

Momentum equation

$$\rho\,(U \cdot \nabla U - f) - \nabla \cdot \sigma = 0 \qquad (2.2)$$

The considered assumptions for 2-D general flow are as follows, Neglected body forces, Uniform isothermal flow, Fully turbulent flow in boundary layer region. The fluid prosperities is homogenous at the initial stage. The working fluid is assumed as perfect gas where the equation of state is: $P = pRT$, the x and y components of the velocity vector are u and v respectively , so for the magnitude of total velocity vector, we have : $|V| = \sqrt{u^2 + v^2}$, The solution of the governing Partial differential equation PDE requires definition of boundary conditions that comply with those PDE, (e.g the no slip condition is associated with viscous flow solution). Furthermore, for those PDE, when approximated by finite different equation FDE, will require more boundary conditions, namely is "numerical" boundary conditions (defining the whole entire domain when using the time marching technique). The boundary conditions for 2-D viscous flow are far-field, downstream and upstream, and viscous wall boundary conditions. Those boundary conditions for 2-D viscous flow are shown in Fig. (2.2):

1- Inflow boundary conditions: all the inflow properties are uniform and specified.

2- Out flow boundary conditions: The Mach number,

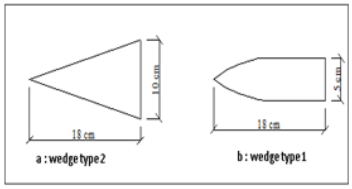

Figure (1) : Studied test wedges type 1 and 2.

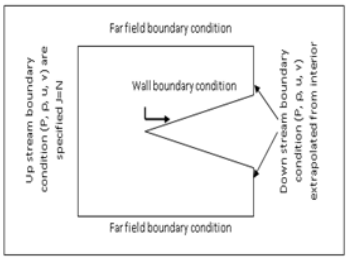

Figure (2) : Schematic diagram showing the identified and calculated boundary conditions.

temperature and primitive pressure are interpolated from the interior points, while the density is calculated from the equation of state

3- The far-filed boundary conditions: All the far-field properties are specified.

4- Wall boundary condition: at the wall the no slip condition imply , that mean u and v are set to be zero at the wall. Additionally, the pressure is calculated from the momentum equation in the y – direction. The momentum equation at the wall is :

$$\frac{\partial P}{\partial Y} = \mu\left(\frac{\partial^2 v}{\partial x^2} + \frac{\partial^2 v}{\partial y^2}\right)$$

But v is approximately zero at the wall, this yields :

$$\frac{\partial P}{\partial Y} = 0$$

The governing equation expressed in vector form and suited for numerical application will be:

$$\frac{\partial U}{\partial t} + \frac{\partial E}{\partial x} + \frac{\partial F}{\partial y} = 0 \qquad (2.2)$$

For inviscid 2-D flow, μ_e considered zero. The governing differential equation will become of the form of Euler equations.

3 Numerical solution procedure

The numerical procedure for subsonic 2-D and viscous flow, the use of h-refinement grid adaption algorithm is used to develop the solution of Navir-Stocks PDE that describes the flow field with the use of coupled control volume solver. Hyperbolic grid generation program built to generate the structured grid for 2-D inviscid flow problem. Then results fed to grid adaption SIERRA program (built in Fortran 99 language) to implement the adaption. And the result show by Tecplote program. The range of numerical program show in table 1.

Table 1. Studied cases

Type of wedge	Angle of attack	Mach Number	Type of Grid
Type 1	0 , -10 , -15 , -20	1.5	With adaption
			Without adaption
		2	With adaption
			Without adaption
		3	With adaption
			Without adaption
		4	With adaption
			Without adaption
Type 2	0	2	With adaption
			Without adaption

4 Verification

The results of adaptation implementation for 2-D supersonic flows will be stated for various Mach numbers and angles of attacks.

Figures (3) to (6) show the non-adapted and adapted grid for various Mach numbers for 2-D supersonic inviscid flows over a wedge of type 1 before and after r-refinement adaption implementation.

All these results are obtained under condition of : ambient temperature of 1200 K and ambient pressure of 1.01325 bar and angle of attack 0, adaption produced a good reduction in computer time where the iteration number is decreased from 3000 to 730. Adaptation resulted in good flow visualization through the resulted adapted grid and one can see the clustering of grid points all over the region of shock wave.

Figures (7) to (9) show the non-adapted and adapted grid for various angles of attacks for 2-D supersonic inviscid flow over a wedge of type 1 before and after r-refinement adaption implementation. All these results are obtained under condition of : ambient temperature of 288.16 K and ambient pressure of 1.01325 bar and Mach number of 1.5, adaption produced a good reduction in computer time where the iteration number is decreased from 3000 to 850. But flow visualization was not good and adaptation relocated the nodes slightly.

Figures (10) to (12) show a set of results for 2-D supersonic inviscid flows over a wedge of type 1. All these results are obtained under condition of: ambient temperature of 288.16 K, ambient pressure of 1.01325 bar, Mach number of 1.5 and angle of attack of 25.

Figures (13) to (14) shows the pressure contours for inviscid flow over a wedge of type 1 and as illustrated on those figures , where figures (15) to (16) shows the velocity vectors for the stated cases. Remarkable iteration number reduction is recorded and more flow visualization noted.

Figures (17) to (21) show a set of results for 2-D supersonic inviscid flow over a wedge of type 2. All these results are obtained under condition of : ambient temperature of 288.16 K, ambient pressure of 1.01325 bar, Mach number of 2 and angle of attack 0. Adaption produced a good reduction in computer time where the iteration number is decreased from 3000 to 1500.

5 CONCLUSIONS

The following conclusion achieved that the Grid adaption showed a great increase in flow solution accuricy which is demonstrated in an increased range of visualized contours regions and new values for in between field parameters recorded for both subsonic and supersonic flows.

Grid adaption was of the same effectiveness for both h-refinement and r-refinement adaption types. Grid adaption was of the same effectiveness for two different studied wedges.

Grid adaption resulted in a good reduction in computer time for 2-D flow problem solution.

Grid adaption successfully visualized flow parameter variation which mean that we can consider the grid adaption as a good flow visualization method.

There is contour regions added for all studied models after adaptation.

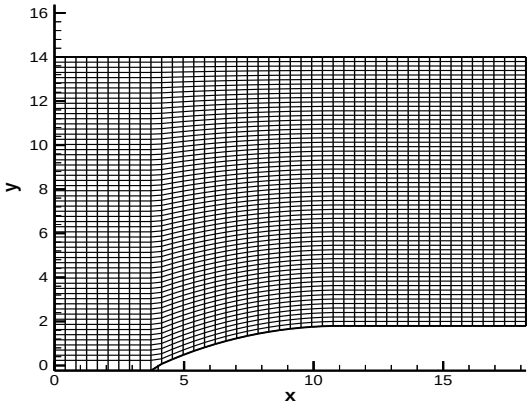

(a) Before adaption

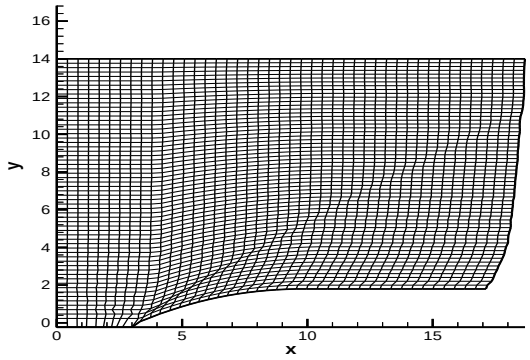

(b) After adaption

Figure (3): Mesh generation at inlet Mach no.=1.5, t_{inf}=1200 K, p_{inf}=101325 Pa, angle of attack=0, t_w=1200 K.

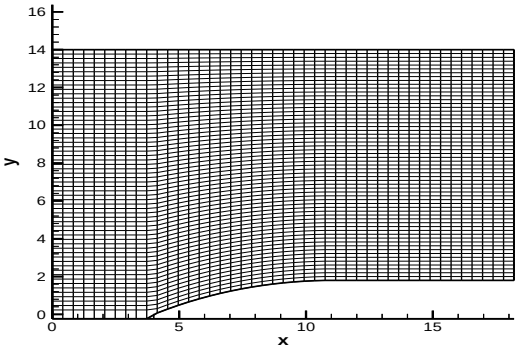

(a) Before adaption

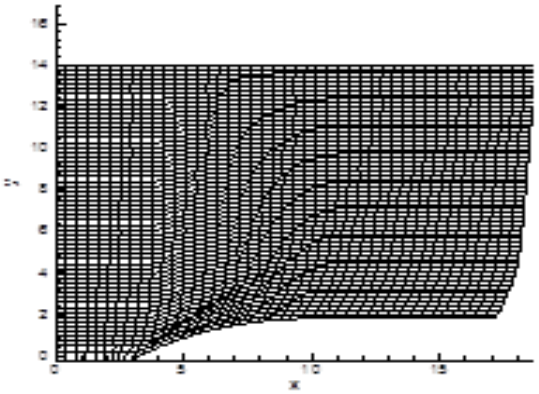

(b) After adaption

Figure (4): Mesh generation at inlet Mach no.=2, t_{inf}=1200 K, p_{inf}=101325 Pa, angle of attack=0, t_w=1200 K.

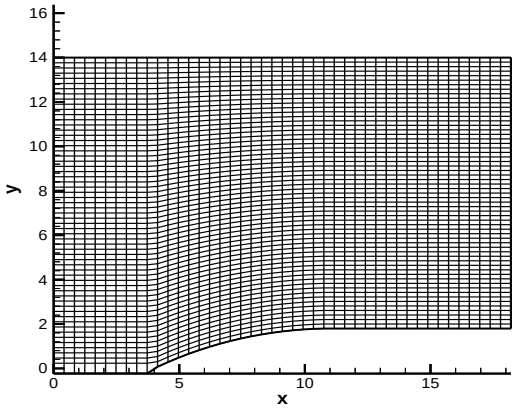

(a) Before adaption

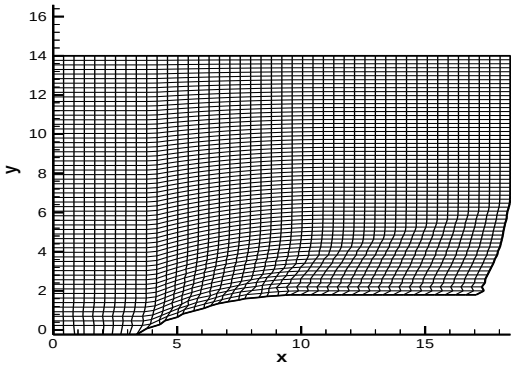

(b) After adaption

Figure (5): Mesh generation at inlet Mach no.=3, t_{inf}=1200 K, p_{inf}=101325 Pa, angle of attack=0, t_w=1200 K.

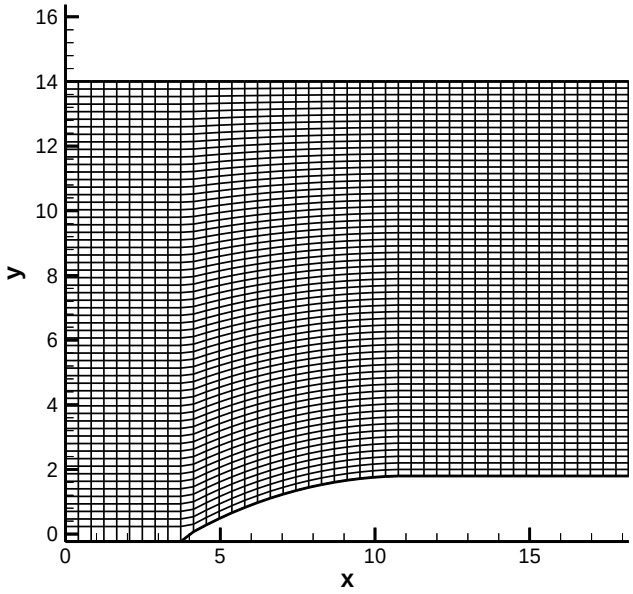

(a) Before adaption

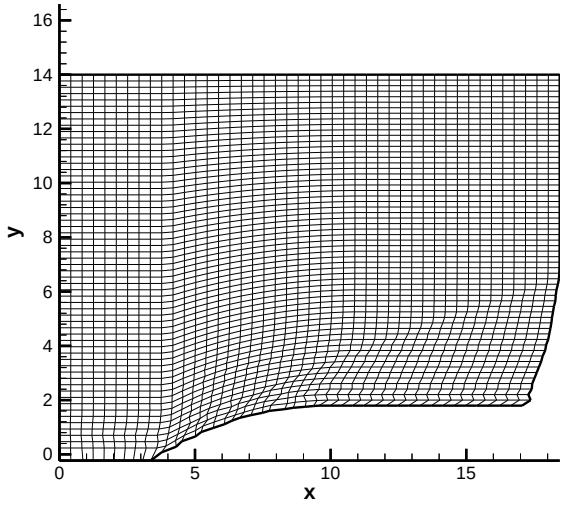

(b) After adaption

Figure (6): Mesh generation at inlet Mach no.=4, t_{inf}=1200 K, p_{inf}=101325 Pa, angle of attack=0, t_w=1200 K .

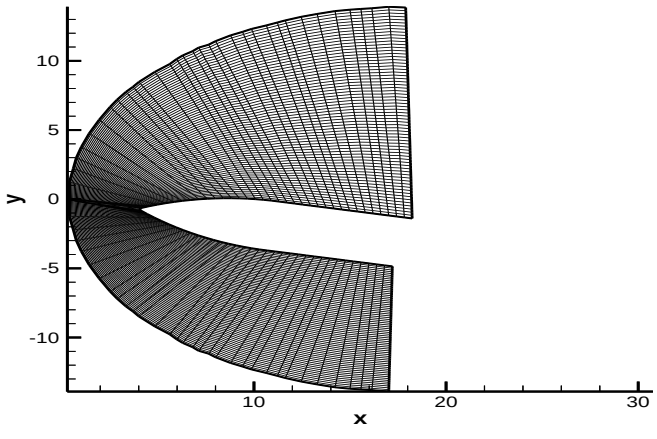

(a) Before adaption

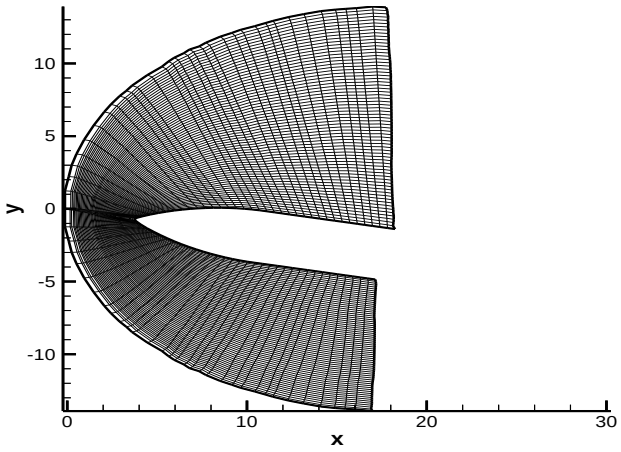

(b) After adaption

Figure (7): Mesh generation at inlet Mach no.=1.5, t_{inf}=288.16 K, p_{inf}=101325 Pa, angle of attack= -10, t_w=288.16 K .

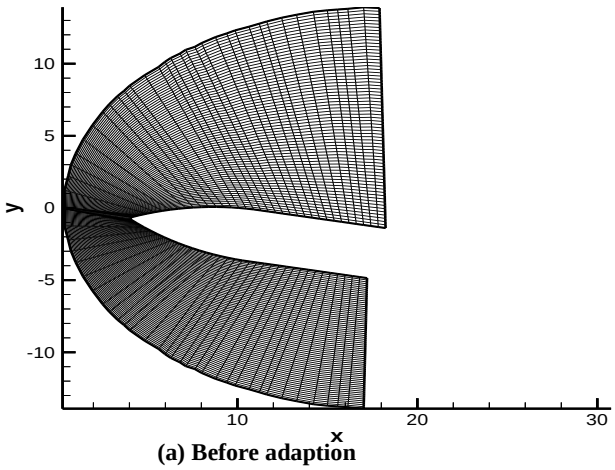

(a) Before adaption

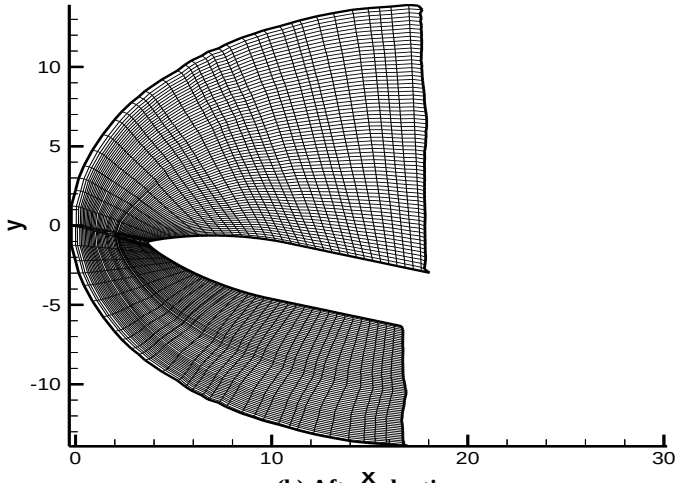

(b) After adaption

Figure (8): Mesh generation at inlet Mach no.=1.5, t_{inf}=288.16 K, p_{inf}=101325 Pa, angle of attack= -15, t_w=288.16 K .

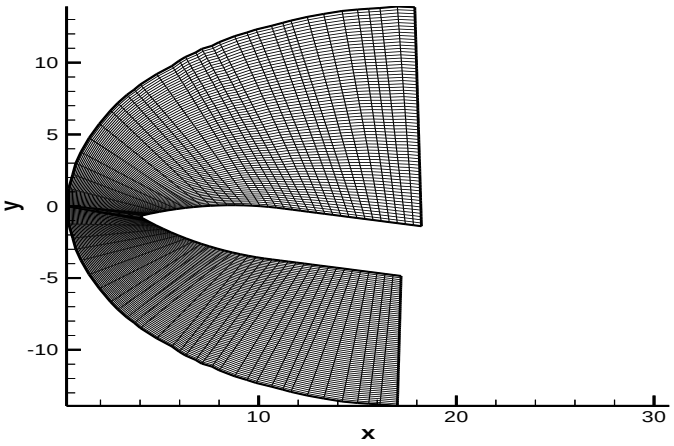

(a) Before adaption

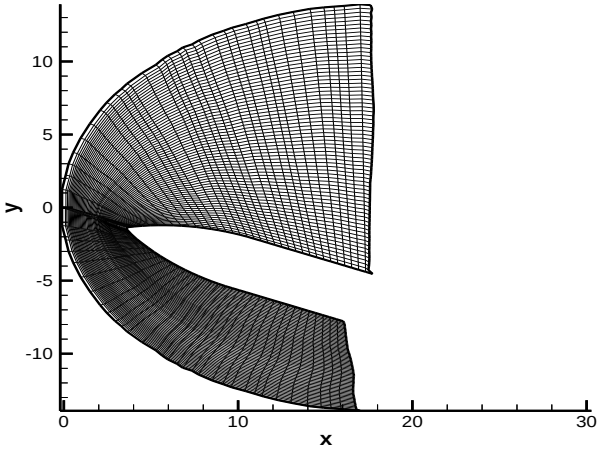

(b) After adaption

Figure (9): Mesh generation at inlet Mach no.=1.5, t_{inf}=288.16 K, p_{inf}=101325 Pa, angle of attack= -20, t_w=288.16 K .

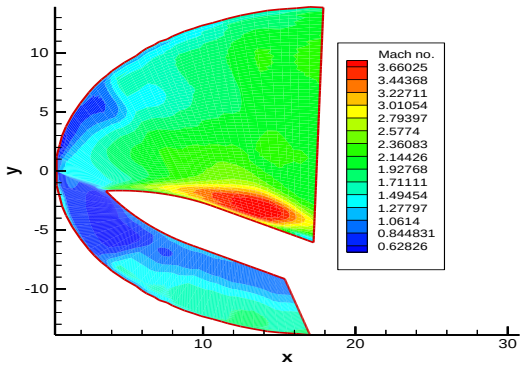

(a) Before adaption, iteration no. =3000

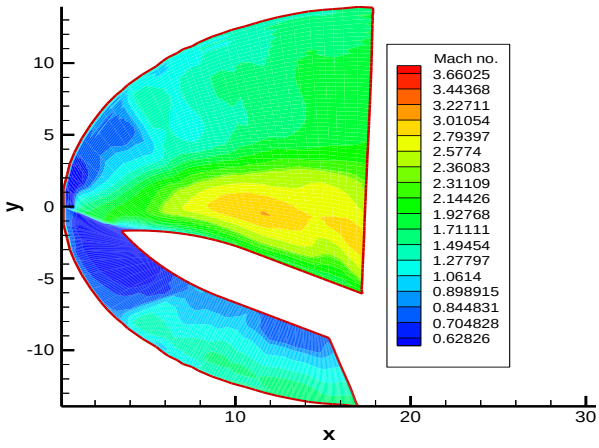

(b) After adaption, iteration no. =850

Figure (10): Mach number contours at inlet Mach no.=1.5, t_{inf}=288.16 K, p_{inf}=101325 Pa, angle of attack= -25, t_w=288.16 K.

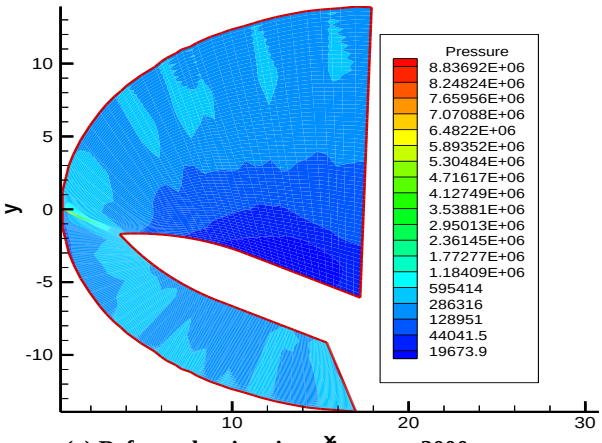

(a) Before adaption, iteration no. =3000

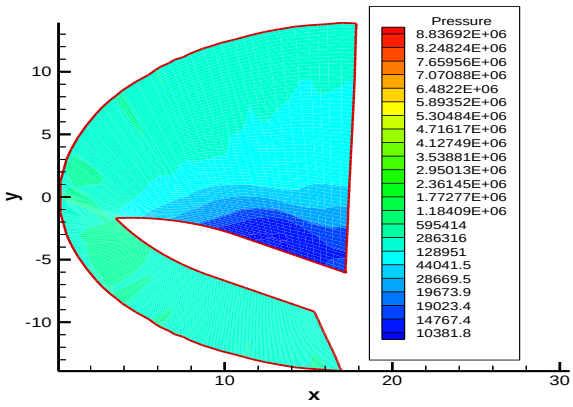

(b) After adaption, iteration no. =850

Figure (11): Pressure contours at inlet Mach no.=1.5, t_{inf}=288.16 K, p_{inf}=101325 Pa, angle of attack= -25, t_w=288.16 K .

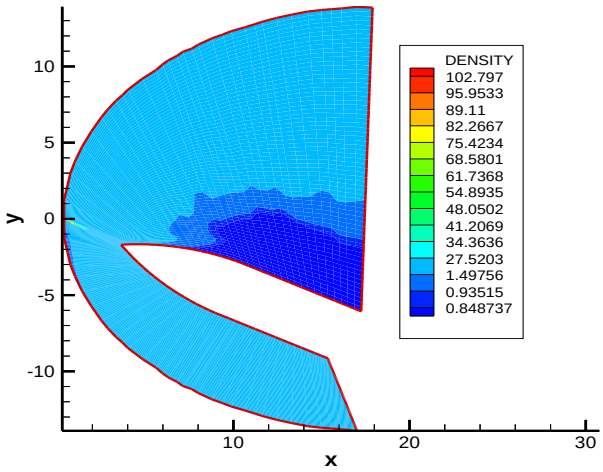

(a) Before adaption, iteration no. =3000

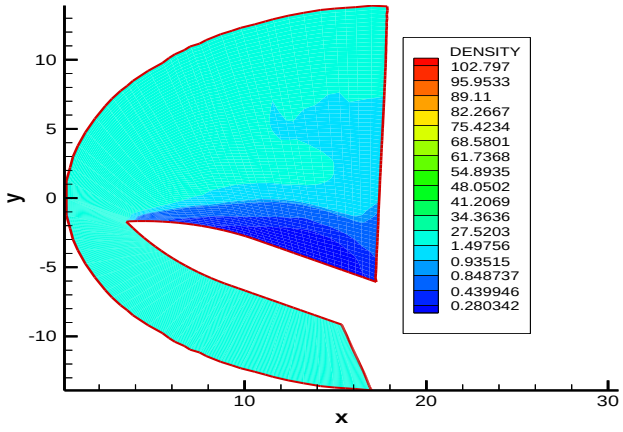

(b) After adaption, iteration no. =850

Figure (12): Density contours at inlet Mach no.=1.5, t_{inf}=288.16 K, p_{inf}=101325 Pa, angle of attack= -25, t_w=288.16 K .

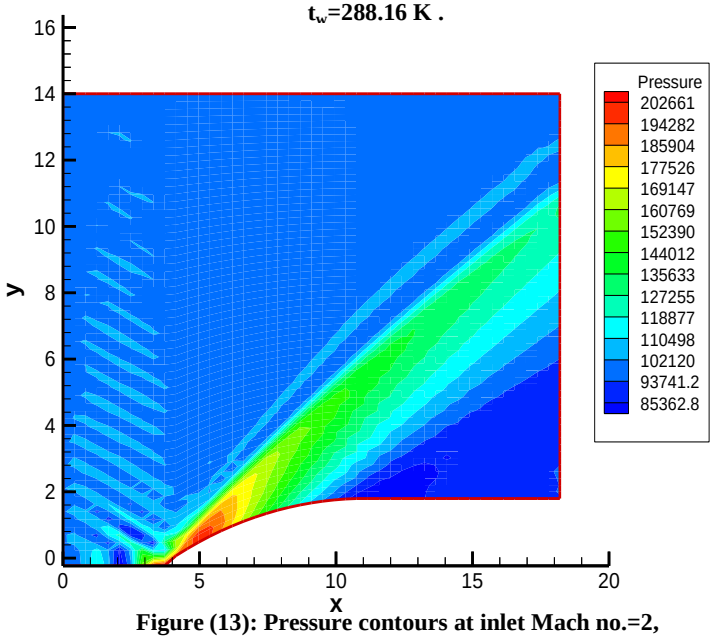

Figure (13): Pressure contours at inlet Mach no.=2, t_{inf}=1200 K, P_{inf}=101325 Pa, t_w=1200 K, iteration=3000 (before adaption).

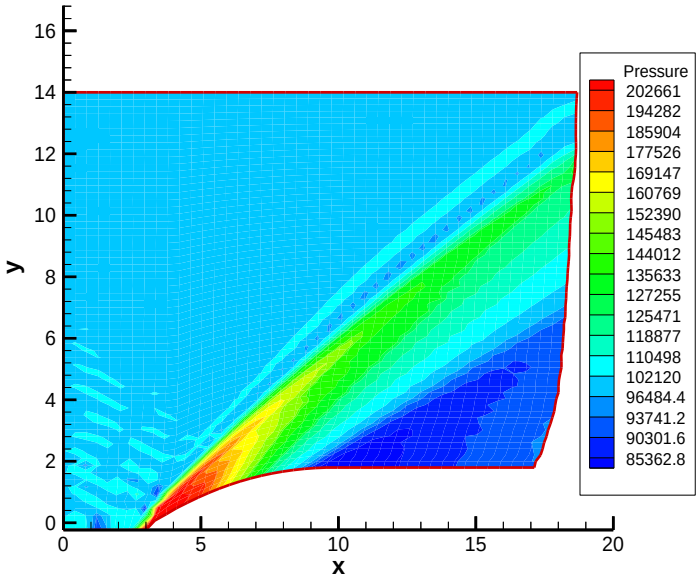

Figure (14): Pressure contours at inlet Mach no.=2, t_{inf}=1200 K, P_{inf}=101325 Pa, t_w=1200 K, iteration=768 (after adaption).

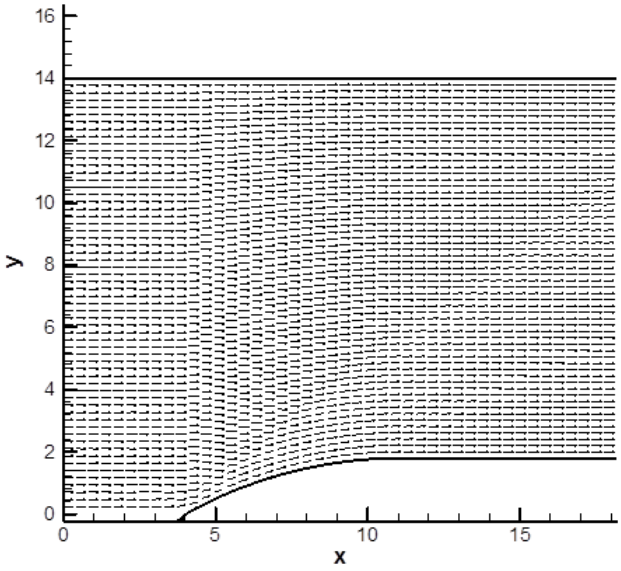

Figure (15): Velocity vectors at inlet Mach no.=2, t_{inf}=1200 K, P_{inf}=101325 Pa, t_w=1200 K, iteration=3000 (before adaption).

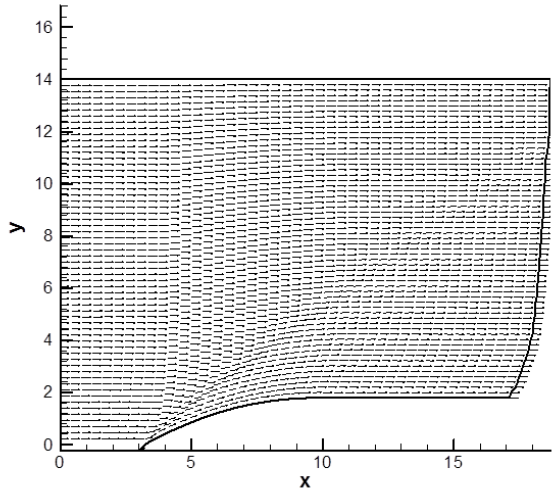

Figure (16): Velocity vectors at inlet Mach no.=2, t_{inf}=1200 K, P_{inf}=101325 Pa, t_w=1200 K, iteration=768 (after adaption).

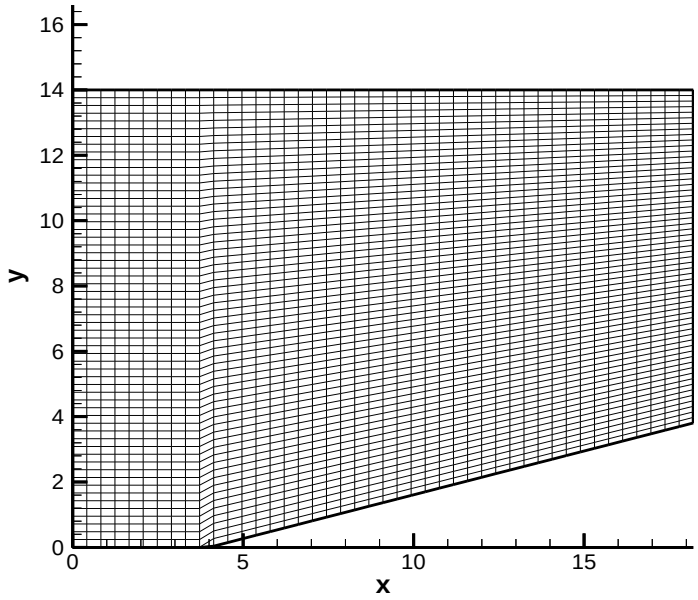

Figure (17): Mesh generation at inlet Mach no.=2, t_{inf}=1200 K, p_{inf}=101325 Pa, angle of attack=0, t_w=1200 K, over wedge no. 2.

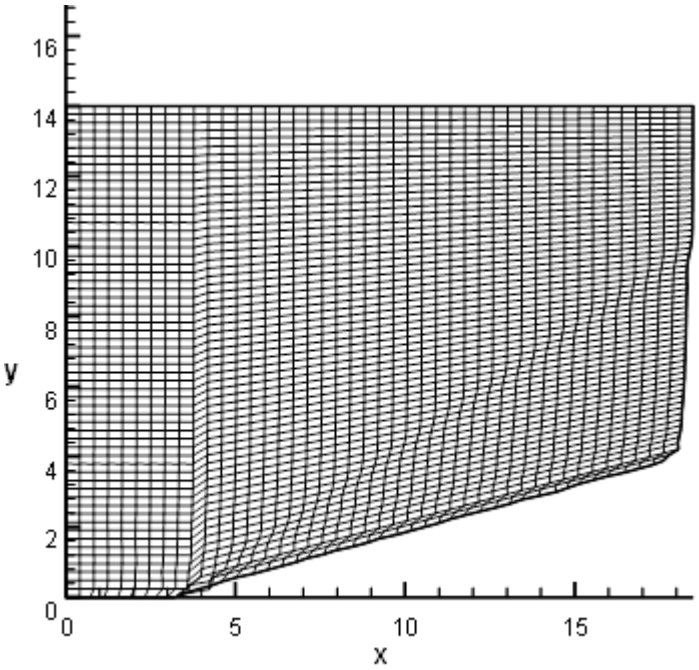

Figure (18): Adapted mesh generation at inlet Mach no.=2, t_{inf}=1200 K, p_{inf}=101325 Pa, alfa=0, t_w=1200 K, over wedge no. 2

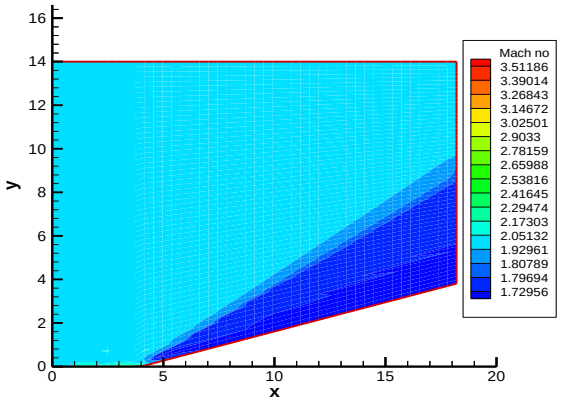

(a) Before adaption, iteration no. =3000

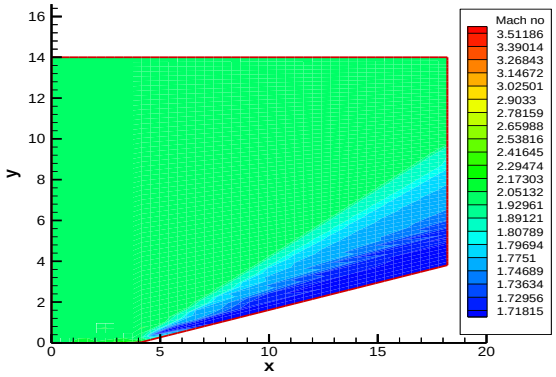

(b) After adaption, iteration no. =1500

Figure (19): Mach contours at inlet Mach no.=2, t_{inf}=1200 K, p_{inf}=101325 Pa, angle of attack=0, t_w=1200 K, over wedge no. 2.

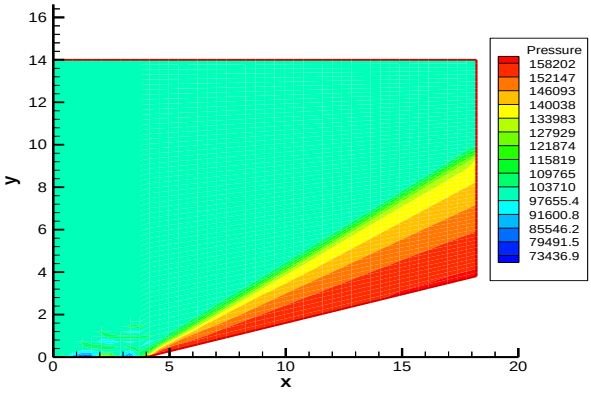

(a) Before adaption, iteration no. =3000

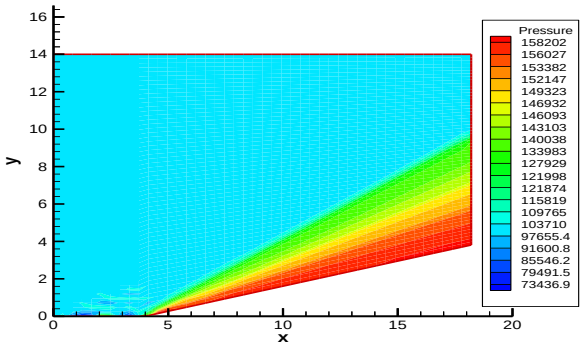

(b) After adaption, iteration no. =1500

Figure (20): Pressure contours at inlet Mach no.=2, t_{inf}=1200 K, p_{inf}=101325 Pa, angle of attack=0, t_w=1200 K, over wedge no. 2.

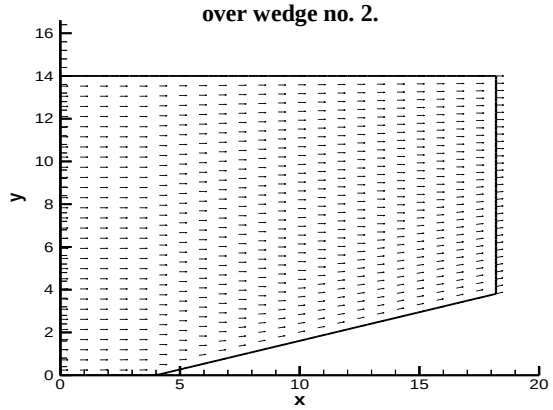

(a) Before adaption, iteration no. =3000

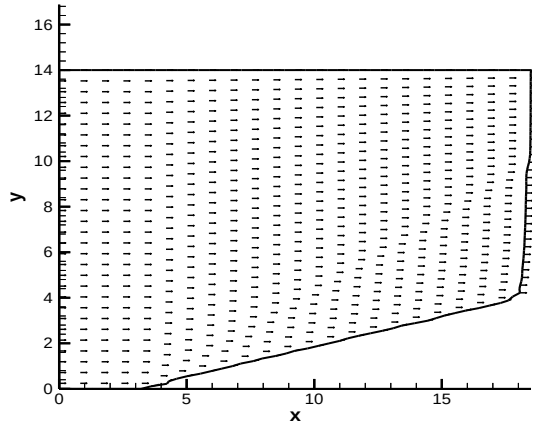

(b) After adaption, iteration no. =1500

Figure (21): Velocity vectors at inlet Mach no.=2, t_{inf}=1200 K, p_{inf}=101325 Pa, angle of attack=0, t_w=1200 K, over wedge no. 2.

6 ACKNOWLEDGMENTS

All praise and thanks are due to my God, the most Compassionate, the most Merciful, and the most Benevolent. My special thanks to my Father and my wife for their support and to all my colleagues and the staff of Mechanical Engineering Department of the University of Baghdad.

7 REFERENCES

1- Berger, M.J. and Antony Jameson, Automatic Adaptive Grid Refinement for the Euler Equations, AIAA Journal, VOL 23, No. 4, April 1985, pp 561-567.

2- Eiseman, Peter R., Alternating Direction Adaptive grid Generation, AIAA Journal, Vol. 23, No. 4, April 1985, pp 551-559.

3- Shen, C.Y. Numerical Simulation of Viscous Flow Using a Solution – Adaptive Method. Ph.D. dissertation, Department of Mechanical Engineering, Arizona State University, Tempe, Arizona, 1991.

4- Borsboom M., Development of an error-minimizing adaptive grid method, Journal of Applied Numerical Mathematics, Vol. 26 (1-2), pp. 13-21, Jan 1998.

5- Littlefield, D. L. – Oden, J. T. and Carey,G.F., Implementation of Adaptive Mesh Refinement into an Eulerian Hydrocode. Jordan Intranet publishes, 2000.

6- Azarenok, B.N. and Ivanenko, A., Application Of Adaptive Moving Grids For Simulation Of Supersonic Gas Flow, J. of computational fluid dynamics, Vol. 10, no. 3, special Issue, pp. 400 – 404, October 2001.

7- Pimentel,C.A.R.-Azevedo, J.L.F.-Figueira da Silva, L.F.-Deshaires,B., Numerical Study Of Wedge Supported Oblique Shock Wave –Obilque Detonation Wave Transitions, journal of Brazilian society of mechanical sciences, Vol.24,no.3, Rio de Janeiro, July 2002.

8- Salih, E.A., Supersonic Flow Over Jet Vane For A Rocket Engine, Ph.D. dissertation, College of mechanical Engineering, Baghdad University, May, 2004.